Cellulose (2024) 31:765–776
https://doi.org/10.1007/s10570-023-05688-6

ORIGINAL RESEARCH

Solvent-free cellulose fatty amide synthesis aided by enzymatic oxidation

Rahul Sharma · Kevin H. Putera · Mark M. Banaszak Holl · Gil Garnier · Victoria S. Haritos

Received: 31 August 2023 / Accepted: 6 December 2023 / Published online: 16 December 2023

Abstract While cellulose is hydrophilic, it is amenable to hydrophobic modification via grafting of its hydroxyl groups. Increased material hydrophobicity could deliver renewable materials with good water barrier properties. This study explores an enzymatic pathway for cellulose fatty amides synthesis. Firstly, we employed the commercially available, low cost enzyme formulation, Cellic® CTec2, to oxidize cellulose under conditions which restricted its hydrolytic enzyme activity. The resulting carboxylated cellulose was reacted with tetradecylamine at 50 °C for 48 h, washed thoroughly with ethanol to give grafted cellulose fatty amides at Degrees of Substitution of 0.57. The formation of cellulose fatty amides was verified by analysis including FT-IR, solid state ^{13}C CP/MAS NMR and Optical Photothermal Infrared Spectroscopy. The hydrophobicity of synthesized cellulose amides was determined by water contact angle (WCA) measurements of disc-compressed fibers; these were significantly increased to $124.3 \pm 12°$ compared with cellulose WCA of $28 \pm 5°$. Additionally, cellulose amide fibers were incorporated into cellulose paper sheets at 10 wt% and gave a remarkable 92% reduction in water droplet area spread compared to plain cellulose sheets. These findings demonstrate the feasibility of enzymatic cellulose oxidation and amidation, and the materials benefits of highly functional cellulose amides which avoid chemical oxidants and reaction solvents.

Keywords Water contact angle · Enzyme processing · Fatty amines · Carboxylated cellulose · Hydrophobicity · Renewable packaging

Supplementary Information The online version contains supplementary material available at https://doi.org/10.1007/s10570-023-05688-6.

R. Sharma · K. H. Putera · M. M. Banaszak Holl · G. Garnier · V. S. Haritos
Department of Chemical and Biological Engineering, Bioresource Processing Research Institute of Australia, Monash University, Melbourne, VIC 3800, Australia

M. M. Banaszak Holl
Department of Mechanical and Materials Engineering, University of Alabama at Birmingham, Birmingham, USA

V. S. Haritos (✉)
Department of Chemical and Biological Engineering, Monash University, Clayton, Australia
e-mail: victoria.haritos@monash.edu

Introduction

Global production of plastics has grown from 2 Mt to 380 Mt since 1950 (Zheng and Suh 2019) and the disposal of much of the plastic waste is limited to incineration or accumulation in landfills, contributing to greenhouse gas emissions and land pollution (Mohanty et al. 2018). Cellulose provides an environmentally sustainable and biodegradable alternative as it is highly abundant with 10^{12} tons produced annually and it is the leading candidate

to replace plastics in many applications (Li et al. 2021). Since cellulose is porous and hydrophilic, it has poor barrier properties allowing water, oil and oxygen to permeate through the surface (Lu et al. 2016). However, packaging materials are required to maintain shelf-life of products by providing barrier protection from moisture, light, dust and microbiological contaminants (Yildirim et al. 2018). For these applications, cellulose can be modified from its native state to imbue such properties (Bethke et al. 2018). For instance, reduced permeation of water and oil for packaging materials could be met by grafting long chain alkyl esters and amides to impart these properties (Huang et al. 2021; Krathumkhet et al. 2021; Liu et al. 2022; Meng and Edgar 2015).

Grafting of functional groups to cellulose can be achieved through reactions at the primary hydroxyl group i.e. C6-OH of the glucose ring, noted to be the most reactive site in the cellulose molecule. Similarly, hydrophobic functional groups have been grafted onto cellulose after carboxylic groups have been generated through oxidation of cellulose fibers with 2,2,6,6-tetramethyl-1-piperidinyloxy radical (TEMPO) (Mendoza et al. 2020). TEMPO oxidation of cellulose has been shown to generate high concentrations of carboxylic acids as sites for amidation as reported in several studies (Benkaddour et al. 2014; Fredrick et al. 2019; Johnson et al. 2011; Krathumkhet et al. 2021; Meng and Edgar 2015). While these studies have shown effective chemical amidation of cellulose, the materials generated were not assessed for barrier properties.

Lytic polysaccharide monooxygenases (LPMO, EC 1.14.99.54), the enzymatic corollary to TEMPO, are oxidoreductase enzymes which oxidize cellulose (Vaaje-Kolstad et al. 2010) and have primarily been employed as isolated enzymes in production of nanocellulose (Chorozian et al. 2022; Han et al. 2021; Koskela et al. 2022; Rossi et al. 2021). However, pure LPMOs are not commercially available for use in materials processing and recombinant production of LPMOs results in very low yields (Gaber et al. 2020) and as such, remain of most value as research tools. Commercially-available formulations like Cellic® CTec2 contain Type III LPMO which oxidizes the cellulose ether bond to form C1 carboxylic acids and C4 gem diols (Bissaro et al. 2017; Müller et al. 2015) but also contains many glucanases with strong cellulose hydrolytic activity. We hypothesized that Cellic® CTec2, in the presence of selective glucanase inhibitors, could be used to generate carboxylic acids on cellulose. This approach is effective and avoids the use of corrosive reactants in comparison to reaction with chloroacetic acid or TEMPO which are used to oxidize cellulose. The carboxylated cellulose fibers are then reacted with a fatty amine to form cellulose amides in solvent-free reaction conditions. To our knowledge, the only solvent free synthesis of amides was performed by Pettignano and Fleury (Pettignano and Fleury 2019) on carboxymethyl cellulose sodium salt with the amine heated just above its melting temperature to impregnate the cellulose powder and reacted at a high temperature of 140 °C. Synthesis of cellulose amides have generally been performed in solvents as in recent publications (Fredrick et al. 2019; Krathumkhet et al. 2021; Meng and Edgar 2015; Yamato et al. 2021). While these studies produce functional cellulose amides, having solvents in the reaction requires rigorous washing for their removal and increases the handling cost from a scale-up point of view indicating the need for solvent-free reaction design.

The goal of this work is to produce cellulose fatty amides using a novel enzymatic pretreatment then amidation under mild conditions, and examine the functional performance of cellulose amides as pure materials and within composite materials. The resulting cellulose fatty amides have potential as hydrophobic renewable materials not only due to the functional properties achieved but also the environmentally benign synthesis route and the biodegradability of cellulose (Insights 2022).

Materials and methods

Chemicals

The cellulose source for the work was never-dried unrefined bleached eucalyptus Kraft (BEK) pulp supplied by Australian Paper, Maryvale at a solids concentration of 10 wt% and composed of neutral sugars in the following range: xylose (8.4–18.9 wt%) and glucose (80–91.5 wt%) with negligible mannose, and will be referred to herein as cellulose fibers. Acetic acid (137130), sodium hydroxide (S5881), 2,6-dimethoxyphenol (D135550), hydrogen peroxide solution (H1009), α-lactose monohydrate

(L3625), L-ascorbic acid (A92902), tetradecylamine (TDA) (T10200), ethanol (L4777), Brilliant Blue G (27815), Nile Red (N3013) and silica gel (94098) were purchased from Sigma-Aldrich (Australia). Whatman Filter paper was purchased from Sigma-Aldrich, Australia. Dilutions of H_2O_2 were made in water directly before use and kept at 4 °C until further use. Homebrand food packaging plastic (PET based) was purchased from a local supermarket.

Enzyme source and activity

Cellic® CTec2 (SAE0020) was purchased from Sigma-Aldrich. It is a cellulase mixture derived from the fungus *Trichoderma reesei*. Enzyme protein content was measured in Costar 96 flat bottom transparent plate adapted for absorbance changes in an Infinite 200 Pro multimode microplate reader Technische Analysegeräte (TECAN, Germany). The Bradford protein quantification method (Bradford 1976) was adapted to determine protein content in the enzyme solution using Bovine Serum Albumin (BSA) as a calibration standard. The protein concentration for Cellic® CTec2 was determined as 204 mg/mL. LPMO activity of the Cellic® CTec2 formulation used 2,6 DMP as the substrate and H_2O_2 as co-substrate to measure activity as previously described (Breslmayr et al. 2018) and resulted in 72 mU/L activity. The enzyme mixture was kept at 4 °C until further use.

Carboxylation of cellulose

Cellulose fibers (5 g dry equivalent) were dispersed in 50 ml of sodium acetate buffer pH 4.8. α-lactose monohydrate (0.27 M) was added to inhibit glucanases together with LPMO reducing agent ascorbic acid (2 mM), and Cellic® CTec2 0.6 µU/g dry fiber (pertaining to 1.7 mg protein/g fiber) were added and the reactions were incubated for 1 to 24 h at 50 °C in a Thermoline incubator without agitation. Lactose was selected as the glucanase inhibitor based on prior research demonstrating competitive inhibition of carbohydrate active enzymes (Fracheboud and Canevascini 1989; Tuohy et al. 2002). Different lactose concentrations were assessed and the optimal concentration provided the highest amount of carboxylic acids on cellulose fibers with least hydrolysis of cellulose. Hydrolytic activities were determined by cellulose mass loss difference measured at the end of the enzyme reaction on oven dried fibers. Post enzyme reaction, the cellulose fibers were washed with 1 L deionised water and filtered under vacuum using a Buchner funnel fitted with a 40 µm filter paper until the solids content was 30% weight basis and measured in triplicate. This material was used thereafter as the substrate for the amidation of carboxylic acids in cellulose. Carboxylic acid concentration of cellulose was determined via conductometric titration and performed using a Mettler Toledo T5 Titrator as described previously (Mendoza et al. 2019).

Amidation of carboxylated cellulose with long chain fatty amine

Carboxylated cellulose fibers (500 mg, ~30 wt% solids) were well mixed with tetradecylamine (500 mg, melting point 37–42 °C) in a 50 ml falcon tube and incubated for 48 h at 50 °C in a Thermoline incubator without agitation. The fibers were filtered to 30 wt% solids to remove free water. In this state the fibers appear dry as most of the water is trapped within the fibre bundles. The amidation reaction is conducted at 50 °C at which TDA is a mobile liquid (melting point ca. 30 °C) allowing access to the cellulose fibers to react with the localised carboxylic acids. Following the amidation reactions, all cellulose materials were thoroughly washed twice with ethanol with centrifugation at 10,000 rpm, 10 min at 20 °C to remove any unreacted material and reclaim fibers. The pelleted cellulose was separated from the supernatant and dried for 48 h in a fume hood to evaporate any residual ethanol. The samples were stored in a desiccator over silica gel.

Cellulose composite papers preparation

Composites were prepared by combining 10 wt% amide functionalised cellulose into unmodified cellulose (90 wt%), that is, 120 mg amidated fibers were mixed with 1.08 g cellulose for 15,000 revolutions using a pulp disintegrator 3 L Mavis Engineering (Model No. 8522). Separately, control cellulose sheets were prepared in an identical manner but contained only 1.2 g cellulose; carboxylated cellulose composite sheets were also prepared with 10 wt% carboxylated cellulose fibers mixed with 1.08 g cellulose. To verify the

composite hydrophobicity, 120 mg carboxylated fibers and 120 mg TDA were admixed and used to prepare similar 10wt% sheets in 1.2 g unmodified cellulose to validate the effectiveness of truly grafted amides. Each solution was made into a handsheet using an Automatic British Handsheet maker (diameter 16 cm) with a 150-size drainage mesh. Whatman Filter paper 541 was used to capture all fibers in the solution. The sheets were pressed twice using an automatic L&W sheet press and conditioned for 24 h at 23 °C and 50% relative humidity as per TAPPI 205 standard method (TAPPI 2002). Additional composite samples were prepared to test the potential for unreacted fatty amine to influence hydrophobicity by combining unreacted tetradecylamine (0.5 g) with carboxylated fibers (0.5 g) and then the resulting fibers were immediately mixed into 10 wt% composites with plain cellulose following the method outlined above, that is, no reaction time between teradecylamine and carboxylated cellulose was allowed and no ethanol washing step was performed.

Materials characterisation

Optical photothermal infrared (O-PTIR) spectroscopy

The Photothermal mIRage Optical Photothermal Infrared (O-PTIR) system (manufactured by Photothermal, Santa Barbara, CA, USA) was used for conducting O-PTIR experiments. The system was equipped with a Quantum Cascade Laser (QCL), enabling data acquisition within the range of 800–1880 cm^{-1}. All experiments were carried out under a N_2 gas purge to maintain 0% relative humidity conditions. IR Spectra were randomly sampled on multiple cellulose fibers from native and Cellic® CTec2 oxidised cellulose samples using the QCL laser with 49% IR laser power and 25% Probe power and are kept consistent across imaging of control and treated sample. Single wavenumber imaging was then collected on multiple cellulose fibers for 1664 cm^{-1} attributed to COO– using 20 × 20 µm region of interest at 0.2 µm pixel density. IR spectra were processed and analyzed using PTIR Studio 4.2 (Photothermal, Santa Barbara, CA, USA). All IR spectra were smoothed using Savitzky–Golay filter with 11 pt smoothing and polynomial order of 3.

ATR-FTIR

FTIR was performed on dried fibers using a Agilent Technologies Cary 630 FTIR coupled with a diamond attenuated total reflectance (ATR) element as described (Mendoza et al. 2020). The resolution of the FTIR was set at 4 cm^{-1} and eight scans were performed per samples in the range of 4000–500 cm^{-1}.

^{13}C solid state CP/MAS NMR spectroscopy

Solid state spectroscopy was performed on dry fibers. All cross-polarization magic angle (CP/MAS) spectra were recorded on a Bruker Avance 300 spectrometer, operating at 75.4 MHz for ^{13}C at a Magic angle spinning rate of 5 kHz at room temperature. A double resonance H/X CP/MAS 4 mm probe was used. For ^{13}C CP/MAS, 24,000 transients were acquired using a contact time of 2.0 ms, an acquisition time of 19.9 ms (1992 data points zero filled to 65 K) and a recycle delay of 4 s. Spectra were referenced using the carbonyl signal of glycine at 176.03 ppm and intensity was normalised for all sample peaks to account for received gain. Calculation of the Degrees of Substitution (DS) was performed using the method outlined by Jandura et al. (2000)

$$DS_{NMR} = \frac{n_{cel} \times I_{ac}}{n_{ac} \times I_{cel}}$$

where I_{ac} and I_{cel} are the integrations of the aliphatic carbon peaks and cellulose carbon peaks respectively and n_{cel} and n_{ac} are the number of carbon atoms in glucose ($n_{cel} = 6$) and carbon atoms in a tetradecylamide moiety ($n_{ac} = 14$).

Water contact angle measurement on cellulose substrate

Unmodified, carboxylated and amidated cellulose fibers were separately pressed onto compression discs of 45 mm using a L&W Press. The surface hydrophobicity of each sample was analyzed using Dataphysics OCA35 instrument as described

previously (Joram et al. 2020). The static contact angle between a water droplet (5 µL, 1 µL/s) and the cellulose surface were measured. Water contact angle of the food grade packaging PET was conducted in parallel with the cellulosic materials.

Drop spread test in 10 wt% paper composites

For water barrier assessment, a solution of Brilliant Blue G (1% w/v) was prepared in Milli Q water and five independent 20 µL drops were pipetted on the prepared 10% (w/w) composite paper sheets. The same test was also performed on admixed composites containing carboxylated fibers and TDA. To determine resistance to oil droplet spread, a solution of Nile Red powder (0.3% w/v) in commercial Canola oil was prepared and tested in a similar manner to the water drop test except, in this case, using 10 µL drops of coloured oil. The area of the blots covered by each drop was calculated via measurement of the drop diameter when dried. Statistical analysis was run in IBM SPSS Statistics 27.0.1. A significance level of 0.05 was chosen for one-way ANOVA analysis and the post hoc Tukey's Honestly significant difference (HSD) test.

Results and discussion

Carboxylation of fibers using Cellic® CTec2

The generation of carboxylate groups on cellulose by Cellic® CTec2 in the presence of lactose, as an inhibitor of glucanases to control excessive hydrolysis, was tested over different incubation times. As shown in Table 1, it was difficult to obtain concentrations of carboxylated groups in cellulose above 25 mmol/kg especially where the reaction was allowed to proceed over longer time intervals. This is most likely due to the preferential hydrolysis of cellulose carboxylic acid groups by glucanases, in agreement with previous studies (Valenzuela et al. 2019; Valls et al. 2019). The optimal conditions were short incubation times of 1–2 h resulting in negligible mass loss of cellulose fibers and cellulose carboxylate content of 25 mmol [COOH]/kg dry fibers based on titration measurements. Given there is negligible mass loss in 1 h incubation with CTec2, cellulose oxidation is highly likely to occur only on the surface chain of the fiber bundles. Cellic CTec2 has been shown to contain mainly hydrolytic enzymes including 15% w/w lytic polysaccharide monooxygenases in a previous study (Müller et al. 2015) and about 20% w/w glucose (Kaabel et al. 2023). Therefore, approximately 65% w/w of the formulation contains other carbohydrate hydrolyzing enzymes. As suggested by the mass loss percentages provided in Table 1, at constant inhibitor concentration, mass loss% increases over time which indicates a diminishing effect of the inhibitor in the reaction. The treatment conditions resulting in 25 mmol/kg carboxylates were selected for further reactions.

Table 1 Concentration of carboxylic acids on cellulose treated with Cellic® CTec2 with glucanases partially inhibited by addition of α-lactose (0.27 M), over different incubation times

Incubation time (h)	[COOH] (mmol/kg dry fiber)	Cellulose mass loss%
1	25	0
2	25	1.4
3	0	11.0
4	20	4.3
5	0	10.4
6	0	11.4
24	0	21.0

The Cellic® CTec2 treated fibers were analyzed by various techniques to verify the production of carboxylic acid groups on the fibers. Spectra obtained from O-PTIR analysis of enzyme treated and unmodified cellulose between 800 and 1800 cm^{-1}, are shown in Fig. 1A. The high-resolution spectra indicated significant absorbance at 1664 cm^{-1} attributed to carboxylate (COO–) groups and at 1736 cm^{-1} associated with carboxylic acid (COOH) groups generated by LPMO in enzyme treated fibers which were absent in the unmodified sample. In Fig. 1B, untreated fibers show a negligible presence of carboxylate groups as the values are close to 0 mV (blue shading) at 1664 cm^{-1}. Conversely, Fig. 1C displays enzyme-oxidized fibers showing substantial voltage readings of 25 mV (green shading) signifying a substantial population of carboxylate groups resulting from controlled enzymatic oxidation. In summary, Cell®CTec2 offers a novel and sustainable approach

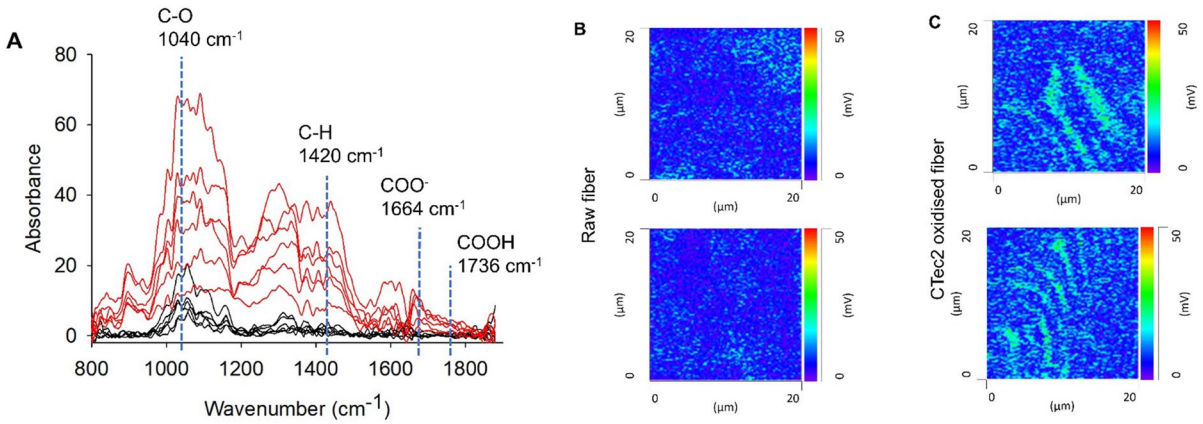

Fig. 1 **A** Optical Photothermal Infrared (O-PTIR) spectroscopy analysis of cellulose fibers by mIRage. Six independent samples are shown for unmodified fiber (black) and Cellic® CTec2 oxidised fibers (red). IR absorbance wavelengths corresponding to characteristic cellulose components are indicated above the spectra. The carboxylic acid and carboxylate stretch absorbance generated by inhibited enzyme samples were detected at 1736 cm^{-1} and 1664 cm^{-1} respectively. **B** mIRage generated chemical maps of unmodified ('raw') cellulose fibers **C** mIRage generated chemical maps of enzyme oxidized fibers. Both **B** and **C** depict the spatial distribution of absorbance at 1664 cm^{-1} in 20 µm square grids at two independent sampling points per sample, allowing for spatial characterization of the cellulose fibers at around 500 nm resolution

for cellulose carboxylation which is a starting point for amide production as illustrated in the reaction scheme (Fig. 2).

Amidation of carboxylated cellulose by reaction with tetradecylamine

After reaction with tetradecylamine, cellulose fiber samples were analysed by Fourier-transform infrared spectroscopy (FTIR) and compared with unmodified and carboxylated fibres. Unmodified fibers exhibited no discernible carbonyl group stretch (black line, Fig. 3A) while Cellic® CTec2 oxidised fibers (red line) displayed a modest carboxylate stretch at 1650 cm^{-1}, quantified as 25 mmol [COOH]/kg fiber by titration (Hu et al. 2018; Koskela et al. 2019). Amidated fibers (blue line, designated regions I–IV) show amide carbonyl stretch absorbance at 1645 cm^{-1} (indicated as III) and amide C–N stretch at 1545 cm^{-1} (indicated as II) (Araki et al. 2001; Barazzouk and Daneault 2012; Benkaddour et al. 2014; Lasseuguette 2008). Additionally, asymmetric and symmetric aliphatic chain stretches were observed at 1460 cm^{-1} and 2800–3000 cm^{-1} (annotated I and IV, respectively) assigned to the fatty hydrocarbon chains. The formation of amides within the enzyme-oxidized fibers was further investigated by ^{13}C solid state CP/MAS NMR (Fig. 3B). The successful transformation of the amine to amide can be clearly seen as the C–N peak stretch in tetradecylamine has been shifted from 1450 to 1545 cm^{-1} in cellulose amide. Furthermore, the characteristic $–NH_2$ peak stretches in amine at 3160 cm^{-1} (asymmetrical), 3250 cm^{-1} (overtone) and 3300 cm^{-1} (symmetrical) are no longer visible in the transformed cellulose amide as the strong and broad –NH– stretch absorbance in the cellulose amide is observed at 3300 cm^{-1} which overlaps with the hydroxyl stretch of cellulose at the same wavenumber. This confirms a change in the chemical environment of the nitrogen. Figure S1 displays the regions I–III and V in a magnified inset. The characteristic aliphatic peaks for the grafted amide were observed between 14 and 35 ppm, while the cellulose pyranose ring carbons are shown from 50 to 110 ppm. A small signal for the carbonyl group was observed at 172 ppm for carboxylated fibers (red) and 163 ppm for the cellulose amide carbonyl group. Calculation of Degrees of Substitution (DS) using the peak integration method revealed a DS of 0.57 for amidated fibers. The spectroscopic analysis provides compelling evidence of successful amidation of enzyme-oxidized fibers, prompting the evaluation of water contact angles and potential applications in paper composites for the cellulose functionalized with fatty chains.

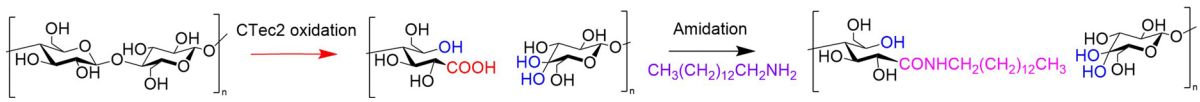

Fig. 2 Step wise reaction schemes for the solvent free Cellic® CTec2-driven synthesis of cellulose carboxylates and cellulose fatty amides

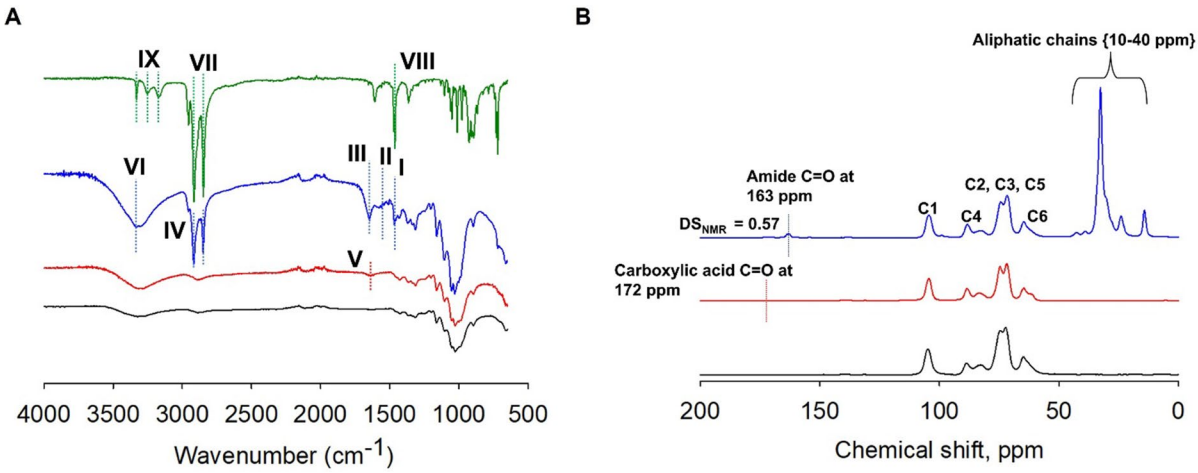

Fig. 3 Spectroscopic analysis of cellulose fiber samples. A. ATR-FTIR spectra of cellulose fiber samples. Marked Regions: I.–CH_2– stretch at 1460 cm^{-1} II. Amide (II) C–N stretch at 1545 cm^{-1} III. Amide (I) C=O carbonyl stretch at 1645 cm^{-1} IV. –CH_2– symmetric stretch at 2800–3000 cm^{-1} V. Carboxylate COO^- stretch at 1650 cm^{-1} VI. NH (amide) and OH (cellulose) stretch at 3300 cm^{-1} VII. –CH_2– symmetric stretch at 2800–3000 cm^{-1} (Tetradecylamine) VIII. C–N stretching at 1450 cm^{-1} IX. –NH_2– stretching at 3160 cm^{-1} (asymmetrical), 3250 cm^{-1} (overtone) and 3300 cm^{-1} (symmetrical) B ^{13}C Solid State CP/MAS NMR spectra of cellulose fiber samples. Legend for spectra: Native cellulose fibers (black), carboxylated cellulose fibers (red), amidated cellulose fibers (blue), tetradecylamine (green, FTIR only)

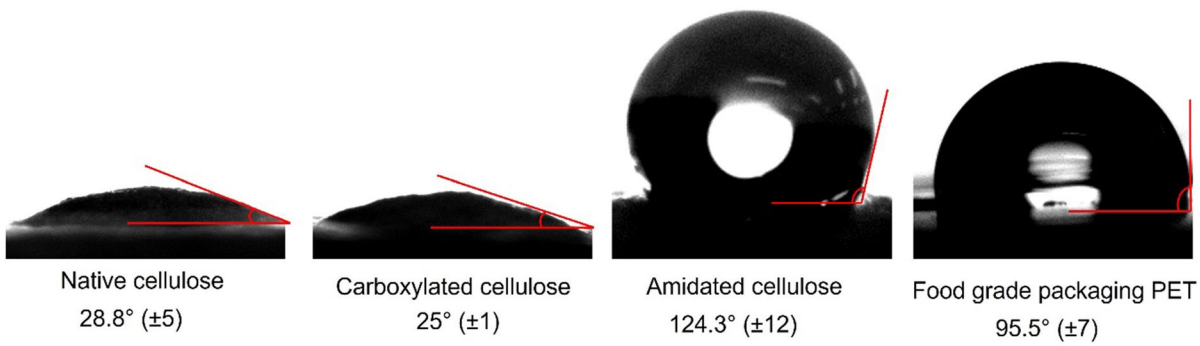

Fig. 4 Water contact angles (WCA) for droplets applied to compressed cellulose fibers to assess hydrophobicity of the surface. Samples included unmodified cellulose, carboxylated cellulose and amidated cellulose. The WCA were compared with a PET packaging material. Standard deviation of five replicates (5 µL drops) is indicated in brackets

Water contact angle and wettability of cellulose amides and their composites

The surface hydrophobicity characteristics of cellulose fatty amides were examined via water contact angle (WCA) of single water droplets. As shown in

Fig. 4, the WCA measurements for unmodified fibers and carboxylated fibers were found to be below 30° on average, consistent with the expected hydrophilic nature of these fibers. Following amidation with tetradecylamine, a significant increase in WCA was observed, with WCA reaching 124.3° for amidated cellulose fibers. This indicates not only a high degree of substitution (DS) on the samples but also effective coverage provided by long-chain alkyl amides on the cellulose surface. The WCA results for amidated fibers align with previous studies that employed long-chain fatty amines for grafting to cellulose (Johnson et al. 2011; Krathumkhet et al. 2021). It is noteworthy to compare our WCA results with that for food-grade plastic, which exhibited a contact angle of 95.5°, almost 30° lower than the amidated cellulose. This finding is consistent with the chemical functionalization of cellulose amide films reported by Krathumkhet et al. (2021) and Johnson et al. (2011) and an improvements over the WCA obtained by Benkaddour et al. (2014).

To further investigate the properties of amidated cellulose, paper composites were prepared to assess hydrophobicity and oil retention functions of the materials, and compare these with unmodified and carboxylated cellulose samples. Composites made of

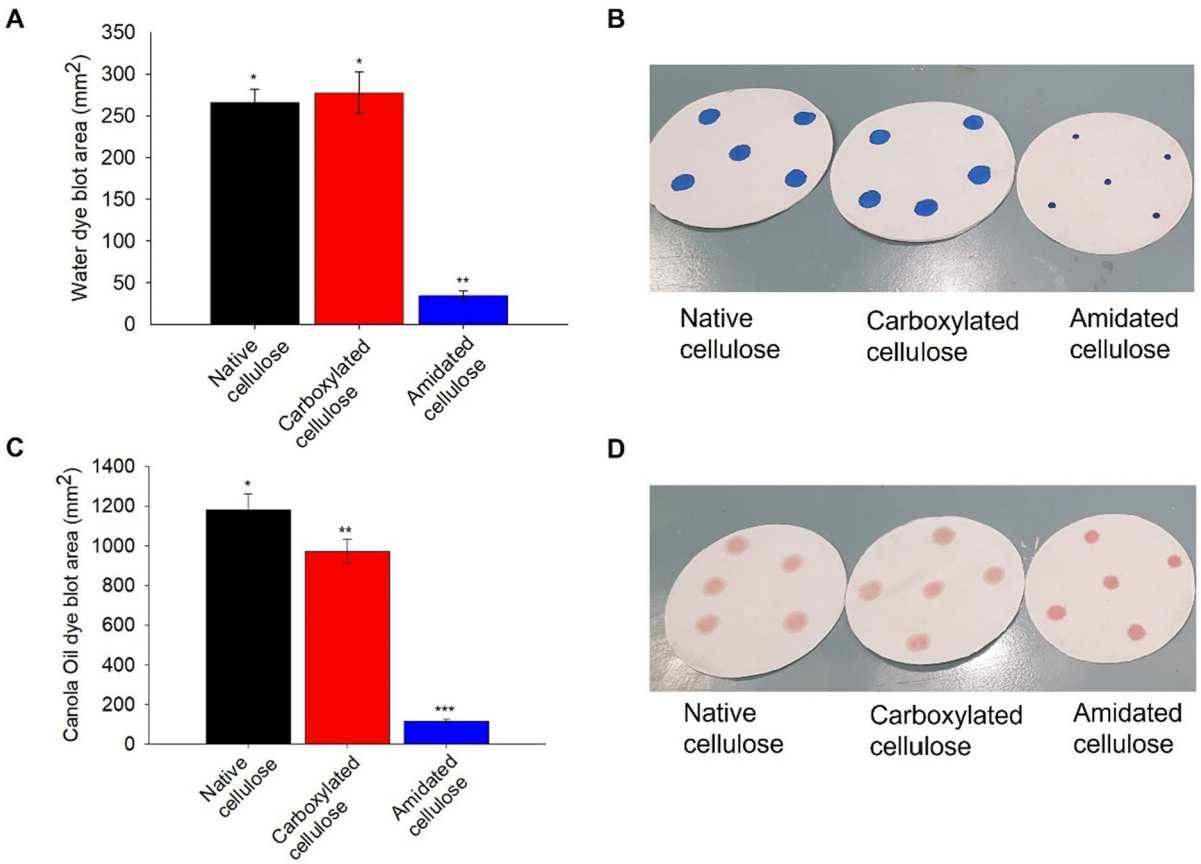

Fig. 5 Assessment of the water and oil resistance of paper composites prepared from a mixture of cellulose amides or carboxylated cellulose or unmodified cellulose blended into a cellulose base at 10% w/w. **A** Area estimate of the spread of water droplets added to the surface of prepared paper composites and **B** image of dried paper composite samples showing the degree of water droplet spread (Brilliant Blue G dye used to delineate the water droplet). **C** Area estimate of the spread of Canola oil droplets added to the surface of prepared paper composites and **D** image of paper composite samples showing the degree of oil droplet spread (Nile Red oil soluble dye used to delineate the droplet spread). Statistical significance levels (denoted with *, **, ***) based on Tukey analysis are indicated to highlight the differences among the tested samples

100% unmodified, and those with carboxylated fibers (10 wt%) added, exhibited similar droplet absorption diameters, attributed to the abundance of hydrophilic groups present in cellulose such as hydroxyls and carboxylic acids in the case of enzyme treated samples. By contrast, composite materials containing amidated cellulose (10 wt%) showed a significant reduction in water droplet diameter, and total droplet areas were reduced by > 90% compared to enzyme-only treated fiber composites (Fig. 5A and B). The increase in material hydrophobicity is attributed to the presence of fatty amides on the fibers, which may impart a homogeneously hydrophobic quality to the composite.

To verify that the composite's hydrophobicity was due to covalently bound fatty amides and not due to adsorbed, unreacted tetradecylamine, a separate composite paper set was prepared by admixing tetradecylamine and carboxylated fibers and immediately forming these into 10wt% paper composites with plain cellulose, without allowing time for reaction and without washing. This composite underwent the same water droplet spread test and showed no difference in area of droplet spread compared with controls (Fig. 6). As can be clearly seen any retained TDA has no functional effect on the surface of the composites as the Coomassie dye water spread is similar to unmodified cellulose therefore verifying that the behaviour observed in Fig. 5A and B is from truly grafted amides on cellulose. Therefore, the admixed composite clearly showed that the extensive hydrophobicity of cellulose amide paper composites shown in Fig. 5 was not due to the presence of retained, unreacted amine.

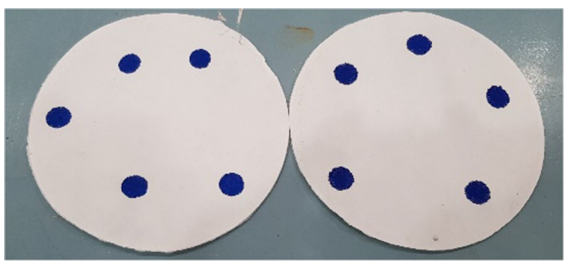

Fig. 6 Composites prepared with 10% (carboxylated fibers + TDA) physical mix to investigate surface hydrophobicity. The image shows the degree of water droplet (20µL containing Brilliant Blue G dye) spread

Another desirable characteristic of renewable packaging is the ability to retain oil on the surface, thereby reducing its spread to the external packaging or internally towards products. To investigate this feature, Canola oil (with Nile Red dye as a tracer) droplets were pipetted onto the surface of the composites and the area of oil spread was estimated and results shown in Fig. 5C and D. Composites containing native and carboxylated fibers exhibited a high spread of oil but those containing amidated cellulose show significantly reduced oil droplet spreading on the surface. This can be attributed to the non-polar character of both the oil and the fatty amides, which are attracted towards each other in the otherwise hydrophilic cellulosic material which prevents its spread. Interestingly, it was observed that the applied oil droplet to cellulose amide composite does not result in the droplet sitting on top of the surface, as it does with water droplets on cellulose amide composites, but rather penetrates directly into the cellulose amide composite. This property warrants further investigation as it differs from the reports obtained by amidation of cellulose using octadecylamine where significant oil repellence was observed in the resulting films (Krathumkhet et al. 2021). However, in the latter case, the cellulose amide films were completely composed of cellulose amides and in our case, only 10% cellulose amide was added to 90% plain cellulose. A study by Geerts et al. (Geerts et al. 2014) has shown that naturally occurring microorganisms, *Pseudomonas aeruginosa* PK1 and *Pseudomonas putida* PK2 can completely mineralize alkyl amides to release ammonium and alkyl acids. On this basis, we expect cellulose amide composite sheets to be completely biodegradable in landfill soils. Thus, our study demonstrates, for the first time, the application of highly functional cellulose amides in paper composites for sustainable packaging products that exhibit strong hydrophobicity and oil retention properties. This work describes a facile and sustainable approach for producing solvent-free cellulose amides firstly using enzymes to carboxylate cellulose and then reacting the intermediate with fatty amines under mild conditions.

Conclusions

The effective synthesis of cellulose amides presents significant sustainability challenges as it has required the use of chemical oxidants, solvents or resulted in low yields due to steric hindrances associated with the cellulose structure. The use of CTec2 for fiber oxidation under conditions that restrict hydrolytic glucanase enzyme activities naturally present in the mixture, is a novel approach to carboxylation of cellulose. The amidation of carboxylated cellulose resulted in DS values of 0.57 in this work, however, the cellulose amides generated were strongly hydrophobic; they exhibited a remarkable increase in water contact angle, reaching up to 124°, surpassing the contact angle of food-grade PET (96°). Here the enzymatic route to cellulose amides is bottlenecked by the low concentration of carboxylic acids generated by Cellic CTec2 under inhibition and further optimization of the CTec2 cellulose oxidation reaction may lead to improved amide conversion. The cellulose amide added at just 10% w/w to paper composites delivered high hydrophobicity and oil retention functionalities to the material This makes long chain cellulose amides ideal for applications where biodegradable papers could replace plastic materials. Further investigation into amidation of cellulose with different-fatty acid chain length of amines may be useful to maximize and tailor functionalized cellulose for different applications such as modulating surface hydrophobicity and oil retention properties.

Acknowledgments We gratefully acknowledge funding from the Australian Research Council-Industry Transformation Research Hub Processing Advanced Lignocellulosics (PALS) [Grant number IH170100020]. We thank Australian Paper Maryvale Mill for providing the Bleached Eucalypt. We thank Dr. Alasdair McKay for his assistance with the ^{13}C CP/MAS NMR experiments at the Monash Analytical Platform Services. We would also like to acknowledge Prof. Florent Allais for his advice on the reaction chemistry of cellulose amide synthesis.

Author contributions RS and VSH: Conceptualization, Methodology, Writing- Reviewing and Editing; KP and MBH: Resources, O-PTIR mIRage, Formal analysis; Writing-Reviewing and Editing GG: Methodology, Writing- Reviewing and Editing; All authors have contributed to writing the manuscript and approved the final draft.

Funding This research was financially supported by the Australian Research Council-Industry Transformation Research Hub (ITRH) Processing Advanced Lignocellulosics (PALS) [grant number IH170100020].

Data Availability Available on request to corresponding author.

Declarations

Competing interests The authors declare no competing interests.

Ethics approval and consent to participate All authors have consented to participate on the manuscript.

Consent for publication All authors approved the final version of the manuscript.

References

Araki J, Wada M, Kuga S (2001) Steric stabilization of a cellulose microcrystal suspension by poly(ethylene glycol) grafting. Langmuir 17(1):21–27. https://doi.org/10.1021/la001070m

Barazzouk S, Daneault C (2012) Tryptophan-based peptides grafted onto oxidized nanocellulose. Cellulose 19(2):481–493. https://doi.org/10.1007/s10570-011-9633-9

Benkaddour A, Journoux-Lapp C, Jradi K, Robert S, Daneault C (2014) Study of the hydrophobization of TEMPO-oxidized cellulose gel through two routes: amidation and esterification process. J Mater Sci 49(7):2832–2843. https://doi.org/10.1007/s10853-013-7989-y

Bethke K, Palantöken S, Andrei V, Roß M, Raghuwanshi VS, Kettemann F, Greis K, Ingber TTK, Stückrath JB, Valiyaveettil S, Rademann K (2018) Functionalized cellulose for water purification, antimicrobial applications, and sensors. Adv Funct Mater 28(23):1–14. https://doi.org/10.1002/adfm.201800409

Bissaro B, Røhr ÅK, Müller G, Chylenski P, Skaugen M, Forsberg Z, Horn SJ, Vaaje-Kolstad G, Eijsink VGH (2017) Oxidative cleavage of polysaccharides by monocopper enzymes depends on H_2O_2. Nat Chem Biol 13(10):1123–1128. https://doi.org/10.1038/nchembio.2470

Bradford M (1976) A rapid and sensitive method for the quantitation of microgram quantities of protein utilizing the principle of protein-dye binding. Anal Biochem 72(1–2):248–254. https://doi.org/10.1006/abio.1976.9999

Breslmayr E, Hanžek M, Hanrahan A, Leitner C, Kittl R, Šantek B, Oostenbrink C, Ludwig R (2018) A fast and sensitive activity assay for lytic polysaccharide monooxygenase. Biotechnol Biofuels 11(1):1–13. https://doi.org/10.1186/s13068-018-1063-6

Chorozian K, Karnaouri A, Karantonis A, Souli M, Topakas E (2022) Characterization of a dual cellulolytic/xylanolytic AA9 lytic polysaccharide monooxygenase from thermothelomyces thermophilus and its utilization toward nanocellulose production in a multi-step bioprocess. ACS Sustain

Chem Eng 10(27):8919–8929. https://doi.org/10.1021/acssuschemeng.2c02255
Fracheboud D, Canevascini G (1989) Isolation, purification, and properties of the exocellulase from Sporotrichum (Chrysosporium) thermophile. Enzyme Microb Technol 11(4):220–229. https://doi.org/10.1016/0141-0229(89)90096-3
Fredrick R, Podder A, Viswanathan A, Bhuniya S (2019) Synthesis and characterization of polysaccharide hydrogel based on hydrophobic interactions. J Appl Polym Sci 136(25):1–7. https://doi.org/10.1002/app.47665
Gaber Y, Rashad B, Hussein R, Abdelgawad M, Ali NS, Dishisha T (2019) Várnai A (2020) Heterologous expression of lytic polysaccharide monooxygenases (LPMOs). Biotechnol Adv 43:107583. https://doi.org/10.1016/j.biotechadv.2020.107583
Geerts R, Kuijer P, van Ginkel CG, Plugge CM (2014) Microorganisms hydrolyse amide bonds; knowledge enabling read-across of biodegradability of fatty acid amides. Biodegradation 25(4):605–614. https://doi.org/10.1007/s10532-014-9685-2
Han X, Bi R, Khatri V, Oguzlu H, Takada M, Jiang J, Jiang F, Bao J, Saddler JN (2021) Use of endoglucanase and accessory enzymes to facilitate mechanical pulp nanofibrillation. ACS Sustain Chem Eng 9(3):1406–1413. https://doi.org/10.1021/acssuschemeng.0c08588
Hu J, Tian D, Renneckar S, Saddler JN (2018) Enzyme mediated nanofibrillation of cellulose by the synergistic actions of an endoglucanase, lytic polysaccharide monooxygenase (LPMO) and xylanase. Sci Rep 8(1):4–11. https://doi.org/10.1038/s41598-018-21016-6
Huang F, Li Q, Ji G, Tu J, Ding N, Qu Q (2020) Liu G (2021) Oil / water separation using a lauric acid-modified, superhydrophobic cellulose composite membrane. Mater Chem Phys 266:124493. https://doi.org/10.1016/j.matchemphys.2021.124493
Insights CM (2022) *Global Hydrophobic Coatings Market Size/Share Worth 3.56 Billion by 2030 at a 4.5% CAGR: Custom Market Insights (Analysis, Outlook, Leaders, Report, Trends, Forecast, Segmentation, Growth)*. https://www.globenewswire.com/en/news-release/2022/10/26/2542063/0/en/Latest-GlobalHydrophobic-Coatings-Market-Size-Share-Worth-3-56-Billion-by-2030-at-a-4-5-CAGR-Custom-Market-Insights-Analysis-Outlook-Leaders-Report-Trends-Forecast-Segmentation-Gr.html
Jandura P, Kokta BV, Riedl B (2000) Fibrous long-chain organic acid cellulose esters and their characterization by diffuse reflectance FTIR spectroscopy, solid-state CP / MAS 13 C-NMR, and x-ray diffraction. J Appl Polym Sci 78(7):1354–1365
Johnson RK, Zink-Sharp A, Glasser WG (2011) Preparation and characterization of hydrophobic derivatives of TEMPO-oxidized nanocelluloses. Cellulose 18(6):1599–1609. https://doi.org/10.1007/s10570-011-9579-y
Joram Mendoza D, Mouterde LMM, Browne C, Singh Raghuwanshi V, Simon GP, Garnier G, Allais F (2020) Grafting nature-inspired and bio-based phenolic esters onto cellulose nanocrystals gives biomaterials with photostable anti-UV properties. Chemsuschem 13(24):6552–6561. https://doi.org/10.1002/cssc.202002017
Kaabel S, Arciszewski J, Borchers TH, Therien JPD (2023) Solid-state enzymatic hydrolysis of mixed PET / cotton textiles. Chemsuschem 16(1):1–8. https://doi.org/10.1002/cssc.202201613
Koskela S, Wang S, Xu D, Yang X, Li K, Berglund LA, McKee LS, Bulone V, Zhou Q (2019) Lytic polysaccharide monooxygenase (LPMO) mediated production of ultra-fine cellulose nanofibres from delignified softwood fibres. Green Chem 21(21):5924–5933. https://doi.org/10.1039/c9gc02808k
Koskela S, Zha L, Wang S, Yan M, Zhou Q (2022) Hemicellulose content affects the properties of cellulose nanofibrils produced from softwood pulp fibres by LPMO. Green Chem. https://doi.org/10.1039/d2gc02237k
Krathumkhet N, Ujihara M (2020) Imae T (2021) Self-standing films of octadecylaminated-TEMPO-oxidized cellulose nanofibrils with antifingerprint properties. Carbohydr Polym 256:117536. https://doi.org/10.1016/j.carbpol.2020.117536
Lasseuguette E (2008) Grafting onto microfibrils of native cellulose. Cellulose 15(4):571–580. https://doi.org/10.1007/s10570-008-9200-1
Li T, Chen C, Brozena AH, Zhu JY, Xu L, Driemeier C, Dai J, Rojas OJ, Isogai A, Wågberg L, Hu L (2021) Developing fibrillated cellulose as a sustainable technological material. Nature 590(7844):47–56. https://doi.org/10.1038/s41586-020-03167-7
Liu S, Liu X, Wang Q, Wang Y, Ji X, Yang G, Chen J, Ni Y (2022) Superhydrophobic, strong and transparent paper made from cellulosic fibers. Cellulose. https://doi.org/10.1007/s10570-021-04393-6
Lu P, Zhang W, He M, Yan Y, Xiao H (2016) Cellulase-assisted refining of bleached softwood kraft pulp for making water vapor barrier and grease-resistant paper. Cellulose 23(1):891–900. https://doi.org/10.1007/s10570-015-0833-6
Mendoza DJ, Browne C, Raghuwanshi VS, Simon GP, Garnier G (2019) One-shot TEMPO-periodate oxidation of native cellulose. Carbohyd Polym 226:115292. https://doi.org/10.1016/j.carbpol.2019.115292
Mendoza DJ, Hossain L, Browne C, Raghuwanshi VS, Simon GP, Garnier G (2020) Controlling the transparency and rheology of nanocellulose gels with the extent of carboxylation. Carbohydr Polym 245(May):116566. https://doi.org/10.1016/j.carbpol.2020.116566
Meng X, Edgar KJ (2015) Synthesis of amide-functionalized cellulose esters by olefin cross-metathesis. Carbohydr Polym 132:565–573. https://doi.org/10.1016/j.carbpol.2015.06.052
Mohanty AK, Vivekanandhan S, Pin JM, Misra M (2018) Composites from renewable and sustainable resources: challenges and innovations. Science 362(6414):536–542. https://doi.org/10.1126/science.aat9072
Müller G, Várnai A, Johansen KS, Eijsink VGH, Horn SJ (2015) Harnessing the potential of LPMO-containing cellulase cocktails poses new demands on processing conditions. Biotechnol Biofuels 8(1):1–9. https://doi.org/10.1186/s13068-015-0376-y
Pettignano A, Fleury E (2019) Solvent-free synthesis of amidated carboxymethyl cellulose derivatives: effect on the thermal properties. Polymers 11(7):1227

Rossi BR, Pellegrini VOA, Cortez AA, Chiromito EMS, Carvalho AJF, Pinto LO, Rezende CA, Mastelaro VR, Polikarpov I (2021) Cellulose nanofibers production using a set of recombinant enzymes. Carbohydr Polym 256:117510. https://doi.org/10.1016/j.carbpol.2020.117510

TAPPI (2002) Forming handsheets for physical tests of pulp. Test Method TAPPI/ANSI T 205 sp-18. Tappi, pp. 1–9

Tuohy MG, Walsh DJ, Murray PG, Claeyssens M, Cuffe MM, Savage AV, Coughlan MP (2002) Kinetic parameters and mode of action of the cellobiohydrolases produced by Talaromyces emersonii. Biochim Biophys Acta Protein Struct Mol Enzymol 1596(2):366–380. https://doi.org/10.1016/S0167-4838(01)00308-9

Vaaje-Kolstad G, Westereng B, Horn SJ, Liu Z, Zhai H, Sorlie M, Eijsink VGH (2010) An oxidative enzyme boosting the enzymatic conversion of recalcitrant polysaccharides. Science. https://doi.org/10.1126/science.1192231

Valenzuela SV, Valls C, Schink V, Sánchez D, Roncero MB, Diaz P, Martínez J, Pastor FIJ (2019) Differential activity of lytic polysaccharide monooxygenases on celluloses of different crystallinity. Effectiveness in the sustainable production of cellulose nanofibrils. Carbohyd Polym 207(November 2018):59–67. https://doi.org/10.1016/j.carbpol.2018.11.076

Valls C, Javier Pastor FI, Roncero B, Vidal M, Diaz T, Martínez P, Valenzuela SV (2019) Assessing the enzymatic effects of cellulases and LPMO in improving mechanical fibrillation of cotton linters. Biotechnol Biofuels 12:1–14. https://doi.org/10.1186/s13068-019-1502-z

Yamato K, Yoshida Y, Kumamoto Y, Isogai A (2021) Surface modification of TEMPO-oxidized cellulose nanofibers, and properties of their acrylate and epoxy resin composite films. Cellulose. https://doi.org/10.1007/s10570-021-04131-y

Yildirim S, Röcker B, Pettersen MK, Nilsen-Nygaard J, Ayhan Z, Rutkaite R, Radusin T, Suminska P, Marcos B, Coma V (2018) Active packaging applications for food. Compr Rev Food Sci Food Saf 17(1):165–199. https://doi.org/10.1111/1541-4337.12322

Zheng J, Suh S (2019) Strategies to reduce the global carbon footprint of plastics. Nat Clim Change 9(5):374–378. https://doi.org/10.1038/s41558-019-0459-z